Journal of Physics:
Conference Series

PAPER • **OPEN ACCESS**

ESEO satellite thermal model design analysis and validation of thermal solutions

To cite this article: A.M Shokry *et al* 2025 *J. Phys.: Conf. Ser.* **3070** 012023

Journal of Physics: Conference Series **3070** (2025) 012023 doi:10.1088/1742-6596/3070/1/012023

ESEO satellite thermal model design analysis and validation of thermal solutions

A.M Shokry[1*], Ahmed Esmat[2], W. M. Elnaggar[3] and Mohamed Elbayoumi[4]

[1] M.Sc., Space Technology Center, Cairo, Egypt
[2] PhD., Astronautics Engineering Department, Military Technical College, Egypt
[3] PhD., Astronautics Engineering Department, Military Technical College, Egypt
[4] PhD., Astronautics Engineering Department, Military Technical College, Egypt

[*]E-mail: Shokryahmed_870@gmail.com

Abstract. This paper focuses on the analysis and investigating the design of thermal control subsystem for a small satellite operating in low Earth orbit (LEO). The European Student Earth Orbiter (ESEO) satellite was selected as the subject of this study. The primary goal of the thermal control subsystem is to guarantee the proper operation against the hard conditions of environment in space. The goal is to certify that the maximum and minimum temperatures of the panel's lower sheet remain within the specified design range. Thermal analysis was implemented using commercially available tools. The comparison between the results showed that maximum Hot Case (1) temperature difference is 2.12 ℃ in panel (3), maximum Hot Case (2) temperature difference is 2.61 ℃ AMSAT. maximum cold Case (3) temperature difference is 1.68 ℃ in SOLAR PANEL (+Z). maximum cold Case (4) temperature difference is 2.05 ℃ in SOLAR PANEL (+X).

Keywords — European Student Earth Orbiter satellite, Thermal control subsystem, Hot worst case, Cold worst case, Thermal Desktop software

1. Introduction

The Thermal Control Subsystem (TCS) is critical for confirming mission success. The major target of TCS is to maintain all spacecraft devices within a reasonable temperature limits [16]. Each device has a range of permissible temperatures that must be sustained to meet survival and operational requirements during mission phases [1].

Thermal control subsystem has many objectives, in which the primary objective is to maintain the temperature of SC devices within a specified limit through rejection of heat dissipated from devices and minimize temperature gradients throughout spacecraft structure to reduce thermal deformations [2]. The devices are scratched if exposed to hot or cold high temperature; Thermal control subsystem is to avoid overheating and undercooling in every part of satellite at satellite mission.

The technology of small satellites has opened numerous new chances in the space part. Different larger systems need significant funding, in the opposite way small satellites offer low funds missions which propagate space industry. Small satellites permit low cost, low risk, and testing of new technologies. This accessibility extends to specialized sectors like as universities, not only developing countries. Additionally, the lower costs also permit administration funding to go farther for research and science plans.

Design thermal control subsystem challenges a for a small satellite grow from some essential properties, as summarized in table (1) [3]. In small satellite because of the constraints of size and volume, there is no enough area to cover the panels by Multi-Layer Insulation (MLI).

Table 1. Small satellite thermal control challenges

Low thermal mass	High responsivity for changing thermal environments.
Limited external surface area	There is restricted space accessible for solar cells and designated radiator areas.
Limited volume	Limited space for electronic components and thermal control hardware, Difficult to isolate different thermal areas.
Limited power	Low power available for active thermal control elements.
Power Density	An important challenge is power dissipation as electronics are arranged close together.

In the United States, small satellite classifications are defined by the National Aeronautics and Space Administration (NASA). Small satellites are commonly defined as less than 180 kg, so there are several subdivisions, as illustrated in Table (2) [4].

Table 2. Small satellite categorizations

Categorizations	Mass [kg]
Minisatellite	100-180
Microsatellite	10-100
Nanosatellite	1-10
Picosatellite	0.01-1
Femtosatellite	0.001-0.01

literature survey explores different methods for the thermal control subsystem to achieve best thermal model solution. Based on literature survey, Thermal control subsystem classified into passive and active elements. Typically, a spacecraft's subsystems undergo multiple design iterations to reach an optimal and possible solution. In some cases, it is needed to change component location and resize radiators several times to meet both the thermal and structural requirements of singular components and the spacecraft as a whole.

In 2022, Ahmed El-Hafnawy published a research paper titled "Passive thermal control design and analysis of a university-class SAT", which explained a different means for the thermal control system to be passive. To support this study, a finite-difference model was developed using a commercial software Thermal Desktop. It was published in Journal of Thermal Analysis and Calorimetry [5].

In 2022, Iwata published a research paper titled "Thermal and Structural Performance of a Small Satellite with Networked Oscillating Heat Pipes", which explained an innovative approach to control heat distribution on structural panel. This method reduces the need to iterate the thermal design process by integrating a network of variable conductance oscillating heat pipes (VC-OHPs) into every structural panel. It was published in journal of spacecraft and rockets. Thermal analysis was conducted using a commercial software package (Thermal Desktop) [6].

In 2021, Tae-Yong Park published a research paper titled “New Thermal Design Strategy to Achieve an 80 kg Class Lightweight X-Band Active SAR Small Satellite S-STEP,” which explained an adjusted thermal control design by decreasing power consumption by adjusting environmental heat fluxes on the satellite and applying a lightweight, flexible graphite sheet as a thermal interface for high-power devices. It was published in the Journal of Aerospace. Thermal analysis was conducted using a commercial software package (Thermal Desktop) [7].

In 2021, Ji-Seok Kim published a research paper entitled “Thermal Model Correlation and Validation of a 6U Nanosatellite with Multiple Payloads”, which explained highlighting the advantages of satellite smallness with lower costs and shorter development timelines. It was published in International Journal of Aeronautical and Space Sciences. Thermal analysis was conducted using a commercial software package (Thermal Desktop) [8].

In 2019, Luis A. Reyes published a research paper titled “Thermal Modeling of CIIIASat Nanosatellite: A Tool for Thermal Barrier Coating Selection,” which evaluated the effects of Thermal Barrier Coatings (TBC) and Orbital Elements (OE) on the internal temperature of a CubeSat nanosatellite. The study applied MATLAB for thermal analysis and was published in an Elsevier journal [9].

In 2018, W. Hengeveld published a research paper titled “Preliminary Design and Comparative Study of Thermal Control in Nanosatellites,” which presented a theoretical analysis of thermal control strategies for nanosatellites. Thermal analysis was conducted using the commercial software Thermal Desktop. The research was presented at the 48th International Conference on Environmental Systems [10].

In 2017, Hemant Ganti published a research paper entitled “Thermal Model and Implementation of Thermal Solutions for Nano Satellite”, which discussed the thermal model of a 2U class Nano-satellite, which takes into account the design parameters including major thermal, heat sinks and the thermal properties of the various materials used in the satellite. It was published in IEEE. Thermal analysis was conducted using a commercial software package (CAD) [11].

In 2015, Andreas Berggren published a research titled “Design of Thermal Control System for the SC MIST”, in which explained the modelling of Multi-Layer Insulation (MLI) using two different approaches, comparing them to determine the necessary level of detail for an accurate MLI model. It was published in Space Conferences and Exposition AIAA space. Thermal analysis was conducted using a commercial software package (Thermal Desktop) [12].

In 2012 research from Politecnico di Milano University, titled “Phase-B Thermal Control Subsystem Design for the ESEO Satellite”, which explained the design of the thermal control subsystem for the ESEO satellite. Thermal analysis was conducted using ESATAN software package [13].

This study introduces different means for the thermal control subsystem for approaching to control radiation heat exchange between the satellite and its environment and Providing the appropriate temperatures for the operation of all subsystems inside the satellite. Overall, to confirm thermal stability, a thermal model is built as the actual model and is simulated in an orbital thermal environment. Thermal model for ESEO satellite has been created using Thermal Desktop software.

The objective of this research is to perform thermal analysis of a small satellite in low earth orbit using a commercial software package is “Thermal Desktop”.

The structure of this work is as follows: first, an overview of the selected satellite for study, ESEO, is provided; next, the thermal analysis model using the nodal lumped parameter method is detailed; finally, the results, discussions, and conclusions are presented.

2. Satellite’s Configuration

The ESEO satellite has a cuboid shape with six panels, including two deployable solar panels and one mounted at panel (1). The main dimensions for ESEO are 967×750×680 mm as like as Figure (1) [13].

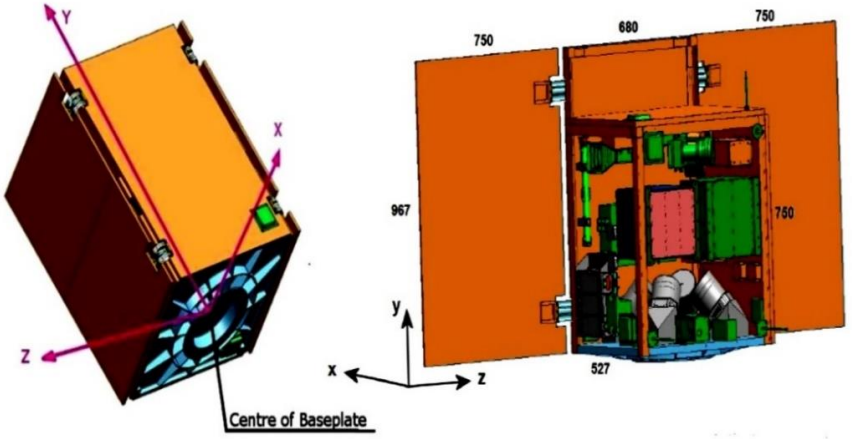

Figure 1. ESEO satellite cuboid shape

The external panels are made of Honeycomb in Aluminium and Aluminium Panels. Aluminium Panels are panel (1), panel (4) and panel (5). Honeycomb panels are panel (2), panel (3) and panel (6). Solar panels are Honeycomb in Aluminium [13].

In this sector we will breakdown ESEO satellite to draw model of the ESEO thermal control subsystem. The entire ESEO satellite was modelled by using Thermal Desktop.

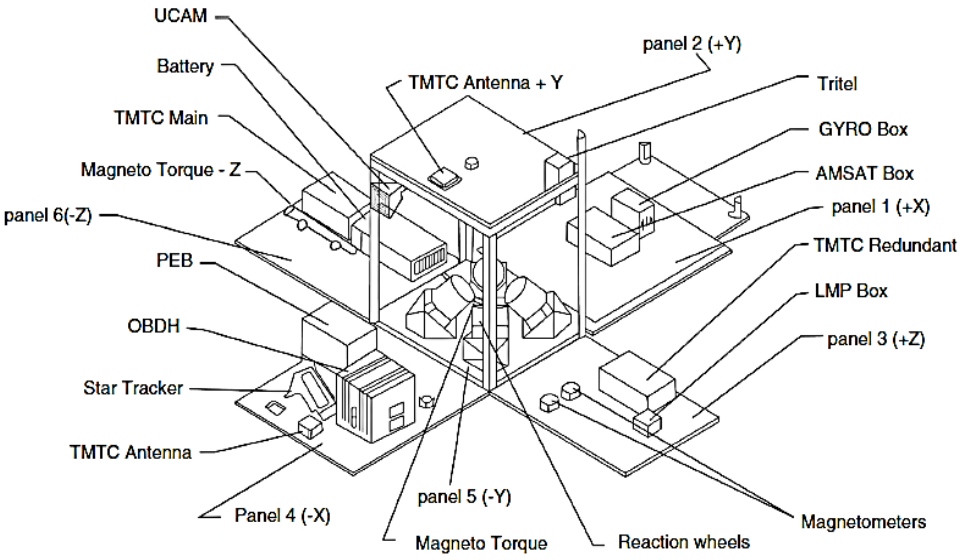

Figure 2. ESEO satellite components

In this section satellite ESEO subsystems will be described as shown in table (3).

Table 3. ESEO satellite subsystems

No.	Component	Subsystem
1	AMSAT	PAYLOAD
2	Tridimensional Telescope dosimeter (TRITEL)	
3	Micro camera (UCAM)	
4	Langmuir plasma diagnostic probe (LMP)	
5	Telemetry and Telecommand system (TMTC)	Communication system
6	Telemetry and Telecommand Antenna (TMTC Antenna)	
7	Electric Power System control unit (EPS PEB)	Electric power system
8	Battery	
9	Reaction Wheel #1, #2, #3, #4	ADCS
10	Magneto Torquer Gyro	
11	Magnetometer #1, #2	
12	Star Tracker	
13	On-Board data Handling (OBDH)	On-board data handling

Orbit for ESEO mission is a sun-synchronous orbit with Local Time of Ascending Node (LTAN) 10:30. The target orbital parameters are listed in the table below. The reference date for the launch is the 01/06/2012 [13].

Table 4. Orbital parameters

Orbital parameters	Symbol	Value
Altitude	a	6898 km
Eccentricity	e	0
RAAN	Ω	47.7° (at nominal launch date)
Argument of periapsis	ω	N/A
Inclination	i	97.48°
True anomaly	θ	Dependent on launch base

3. TCS Design Procedure [14]

- Detect the devices (at least the most sensitive items):
  1. Define satellite geometry and dimensions.
  2. Collect device data information (dimensions, mass and thermal capacity, thermal conductivity of materials, joints and surface thermo-optical properties).
  3. Define thermal requirements like as heat dissipation based on operational mode.
- Perform a thermal analysis to predictable temperature area evolution:
  1. Identify changing in thermal environment and heat paths between devices.
  2. Assume default values for undetermined characteristics from previous experience.
  3. Define scenarios for thermal worst cases.
  4. Create a thermal mathematical model (TMM) for parametric simulation.
  5. For consistency check the solution.

- Suggest appropriate design:
  1. Suggest a basic solution to be integrated into the overall spacecraft design (size of radiator and design, heaters, mass and power budgets, and special TCS elements.
  2. Propose enhancements to the essential solution, considering interactions of TCS with other subsystems.
  3. Iterate with new inputs from the other subsystems, and propose solutions to emerging issues.
- Ensure the design:
  1. Propose on-board thermal control diagnostics to observe suitable operation during tests and flight operations. Plan to detect irregular behaviour.
  2. Verify expectations with tests, and improve the design if desired.

4. Thermal Energy Balance

An important step in the thermal control process is to determine how much heat is absorbed, stored, generated and dissipated by the spacecraft [15]. The thermal design guarantees that in orbit, which is verified through analysis, modelling, and testing. Satellite thermal control in orbit is done via equivalent balance between the absorbed heat and internal heat generated to release heat to space [17]. This model is divided into nodes. These nodes transfer heat between each other via conduction and radiation. This thermal energy balance equation for node i coupled with node j through N is given by [14]:

$$C\frac{\mathrm{dT}_i}{\mathrm{dt}} = \dot{\mathrm{Q}}_{\mathrm{int}} + \dot{\mathrm{Q}}_{\mathrm{ext}} + \sum_{\substack{j=1 \\ j\neq 1}}^{N} \dot{\mathrm{Q}}_{\mathrm{ij}} \quad (1)$$

where; C is overall thermal capacity [J/K]; $\dot{Q}_{int}$ is the internal loads [W]; $\dot{Q}_{ext}$ is the external loads [W].

The term $\dot{Q}_{int}$ is the devices heat dissipated during operating phase can be calculated by summation the heat dissipated from devices through operating phase during mission.

The term $\dot{Q}_{ext}$ is the external loads like as solar, albedo, planetary heat rate and node heat output to space, which can be calculated by;

$$\dot{Q}_{ext} = \dot{\mathrm{Q}}_{\mathrm{s}} + \dot{\mathrm{Q}}_{\mathrm{a}} + \dot{\mathrm{Q}}_{\mathrm{p}} - \dot{\mathrm{Q}}_{\infty,\mathrm{i}} \quad (2)$$

where; $\dot{\mathrm{Q}}_{\mathrm{s}}$ is solar heat input [W]; $\dot{\mathrm{Q}}_{\mathrm{a}}$ is albedo heat input [W]; $\dot{\mathrm{Q}}_{\mathrm{p}}$ is planet heat input [W]; $\dot{\mathrm{Q}}_{\infty,\mathrm{i}}$ Node heat output to space [W].

The term $\dot{Q}_{s}$ can be calculated by:

$$\dot{\mathrm{Q}}_{\mathrm{s}} = A_{pr}\alpha_s S \quad (3)$$

where; A_{pr} is the projected area [m^2]; α_s is the absorptivity of external panels; S is the solar constant (Solar flux).

The term $\dot{Q}_{a}$ can be calculated by:

$$\dot{\mathrm{Q}}_{\mathrm{a}} = A_{pr}\alpha_s S F_{S-E} f \cos\theta \quad (4)$$

where; F_{S-E} is the view factor from the satellite to the Earth; f is the albedo factor; θ is the angle between the satellite position and the zenith.

The term $\dot{Q}_p$ can be calculated by:

$$\dot{Q}_{\mathrm{p}} = A_{pr} F_{S-E} \varepsilon G \tag{5}$$

where; ε is the emittance of external surfaces; G is Earth's radiation flux [W].

The term $\dot{Q}_{\infty,i}$ can be calculated by:

$$\dot{Q}_{\infty,i} = \sigma \varepsilon A_i T_i^4 \tag{6}$$

where; σ is Stefan-Boltzmann constant [5.67×10^{-8} W/m^2.K^4]; ε is emissivity factor; T is temperature of node [K].

The Term $\sum_{\substack{j=1 \\ j\neq1}}^{N} \dot{Q}_{\mathrm{ij}}$ is The heat input to node i by conduction and radiation. This is can be calculated by;

$$\sum_{\substack{j=1 \\ j\neq1}}^{N} \dot{Q}_{\mathrm{ij}} = \sum_{\substack{j=1 \\ j\neq1}}^{N} \dot{Q}_{\mathrm{cond,ij}} + \sum_{\substack{j=1 \\ j\neq1}}^{N} \dot{Q}_{\mathrm{rad,ij}} = \left[\sum_{j=1}^{N} K_{ij}\left(T_i - T_j\right) + \sum_{j=1}^{N} R_{ij}\left(T_i^4 - T_j^4\right)\right] \tag{7}$$

The term K_{ij} can be calculated by:

$$K_{ij} = \frac{k_{ij,eff} A_{ij,eff}}{L_{ij,eff}} \tag{8}$$

where; K_{ij} is the conductance between nodes; $k_{ij,eff}$ is an effective conductivity of the materials implied [W/m.K]; $A_{ij,eff}$ is an effective heat-flow area [m^2]; $L_{ij,eff}$ is an effective distance between nodes [m].

The term R_{ij} can be calculated by:

$$R_{ij} = A_{ij,eff} F_{i-j} \varepsilon_{ij} \tag{9}$$

where; R_{ij} is the radiative coupling [W/ K^4]; F_{i-j} is view factor between nodes i and j; ε_{ij} is emissivity between nodes i and j.

5. Geometry Creation

The First stage in drawing the model is the determination of the external geometry. The spacecraft feature is a cuboids' structure consist of six structural panels and three solar panels, one fixed and two deployable. In the Thermal Desktop software, all the panels were drawn as a rectangle. Based on ESEO design, the external panels are made of honeycomb and aluminium 2024. Aluminium was used for panels one, four, and five, positioned in the +X, -X, and -Y directions, respectively. Based on ESEO design, these aluminium panels have a thickness of 20.6 mm. Honeycomb panels were utilized for panels two, three, and six, located in the +Y, +Z, and -Z directions, respectively [13]. Three solar panels utilized Honeycomb panels. The thickness of equipment panels is of 20.6 mm, while the thickness of solar panels is 13.6 mm [13].

The second stage includes describing the internal geometry that characterises equipment inside the satellite. In the Thermal Desktop software, all internal equipment was drawn as cylindrical or box-shaped symbols. The thickness of each component was assigned 5 mm, a heat capacity is Cp = 921 J/kg·K, and a thermal conductivity is k = 155 W/m. K [13]. Figure 3 shows the final representation of the ESEO spacecraft geometry as modelled in the Thermal Desktop.

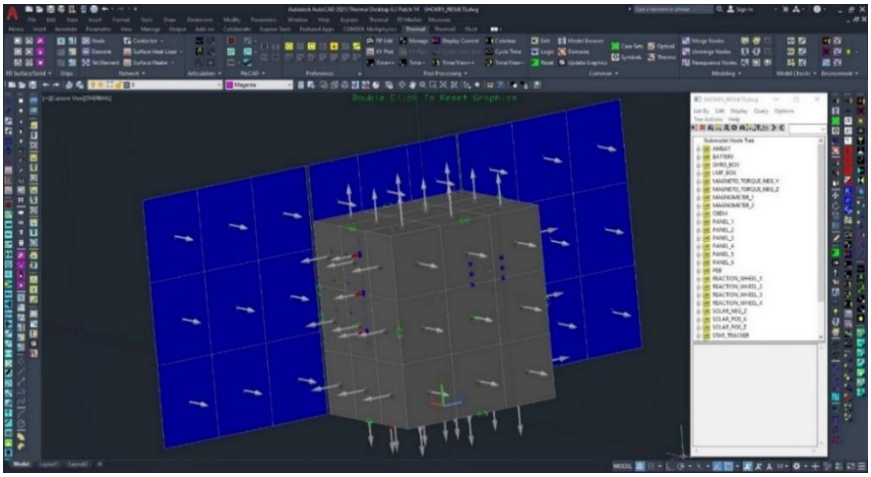

Figure 3. ESEO spacecraft geometry as modelled in the Thermal Desktop

The optical properties of the internal satellite components, the inner surfaces of the structural panels and external optical properties were chosen as specified in table 5. The thermo-physical properties of the structural panels, solar panels, and internal equipment are detailed in table 6, table 7, and table 8, respectively [13].

Table 5. Optical Properties

Material	Panel	Type	α	ε
MLI	Panel 1,3,4,6	Insulation	0.55	0.78
Aeroglaze A276 white paint	Panel 2	Coating	0.26	0.88
Teflon Aluminized 1 mm	Panel 5	Radiator	0.14	0.6
Silver Teflon	Solar panels front side	Tape	0.08	0.78
Solar cells	Solar panels front side	Cells	0.92	0.85
AMJ-750-LSBU	Solar panels front side	Coating	0.76	0.81
Aluminium finish polished surface	Internal components	Coating	0.15	0.05

Table 6. Structural panels thermos-physical properties

Panel No	Material	Volumetric Density [kg/m^3]	Specific Heat Cp [J/kg·K]	Conductivity [W/m·K]
Panel 1	Aluminium	522.878	921	155
Panel 2	Honeycomb	725.701	921	97.857
Panel 3	Honeycomb	791.074	921	97.857
Panel 4	Aluminium	541.292	921	155
Panel 5	Aluminium	1177.37	921	155
Panel 6	Honeycomb	707.123	921	97.857

Table 7. Solar panels thermos-physical properties

Panel No	Material	Volumetric Density [kg/m^3]	Specific Heat Cp [J/kg·K]	Conductivity [W/m·K]
Solar +X	Honeycomb	503.953	921	155
Solar - Z	Honeycomb	503.953	921	97.857
Solar +Z	Honeycomb	503.953	921	97.857

Table 8. Internal equipment thermo-physical properties

Component	Shape	Mass [kg]	Volume×10^{-6} [m^3]	Volumetric Density [kg/m^3]
AMSAT box	Box	0.72	695	1035.98
TMTC Redundant	Box	4.61	836	5514.35
TMTC antenna +X	Box	0.12	198.12	605.69
OBDH	Box	12	1445.31	8302.72
EPS PEB	Box	8.4	1491.5	5631.91
Star tracker	Box	2.06	341.472	6032.7
TMTC antenna -X	Box	0.12	198.12	605.69
Reaction Wheel	Box	0.96	2617.25	366.8
UCAM	Box	0.72	222.405	3237.34
Magneto-Torquer +Y	Cylinder	1.44	12.4056	11607.66
TMTC Antenna +Y	Box	0.12	198.12	605.69
Reaction wheel 1	Box	1.8	977.75	1840.96
Reaction wheel 2	Box	1.8	977.75	1840.96
Reaction wheel 3	Box	1.8	977.75	1840.96
Reaction wheel 4	Box	1.8	977.75	1840.96
Magneto_Torquer -Y	Cylinder	1.44	12.4056	11607.66
TRI-TEL S	Box	1.44	110.39	13044.66
TMTC Antenna + Y	Box	0.12	198.12	605.69
TMTC box	Box	4.61	836	5514.53
Gyro box	Box	1.8	386.32	4659.35
Magnetometer 1	Box	0.07	727.5	962.2
Magnetometer 2	Box	0.07	727.5	962.2
TMTC Antenna +Z	Box	0.12	198.12	605.69
EPS Battery	Box	7.98	6035	1322.29
LMP	Cube	0.96	192	5000
Magneto_Torquer - Z	Cylinder	1.44	12.4056	11607.66
TMTC Antenna -Z	Box	0.12	198.12	605.69

A total of nine nodes were given to each panel, resulting in 81 nodes for the main structural panels and solar panels. Moreover, each internal equipment component was represented by six nodes, adding up to 126 nodes, to be the total number of nodes in the numerical model to 207. Commonly, increasing the number of nodes improves the resolution of the results; however, it also adds complexity to the model and requires long time for computation.

Once the model is defined and initial conditions are established, both steady-state and transient thermal computations can be completed for all nodes over the specified time interval.

6. Boundary and operating conditions

Spacecraft thermal loads can be classified to external and internal heat loads. External heat loads refer to orbital condition as shown in table (9) and Internal heat loads refer to heat dissipation from satellite components in operational modes as shown in table (10 to 13) [13]. The design strategy is to study the two risky cases defined as:

Hot Worst-Case (HWC): refers to the maximum external and internal heat loads. Internal heat loads can be calculated by internal heat dissipation for components at (Mode: 19) [13].

Cold Worst-Case (CWC): refers to the minimum external and internal heat loads operational mode. Minimum internal heat dissipation for components at (Mode: 24) [13].

The internal components consume electrical power which is converted to heat. By evaluating the dissipated power from table of modes, it is obvious that in mode 19 most dissipated power generated by the internal components (177 W) [13], while in mode 24 the minimum power dissipation (60.12 W) [13]. By taking into account that mode 1 is the least dissipated power (0 W), but this mode occurs once the satellite is still on ground or not launched.

Table 9. Orbital Conditions

Item	Hot Case	Cold Case
Solar radiation (W/m^2)	1418	1326
Earth radiation (W/m^2)	258	208
Albedo	0.35	0.25

Table 10. Operational modes [Dissipated Power Modes 1-8]

Component	Mode1	Mode2	Mode3	Mode4	Mode5	Mode6	Mode7	Mode8
AMSAT box	0	0	0	0	0	0	0	0
TMTC Redundant	0	0	0	0	0	0	0	0
TMTC antenna +X	0	0	0	0	0	0	0	0
OBDH	0	30	30	30	30	30	30	30
EPS PEB	0	12	12	12	12	12	12	12
Star tracker	0	0	0	0	0	0	0	0
TMTC antenna -X	0	0	0	0	0	0	0	0
Reaction Wheel	0	0	0	0	0	0	0	0
UCAM	0	0	0	0	0	0	0	3.6
Magneto-Torquer +Y	0	1.2	1.2	3	3	2.16	2.16	0
TMTC Antenna +Y	0	0	0	0	0	0	0	0
Reaction wheel 1	0	0	0	0	0	6	6	14.4
Reaction wheel 2	0	0	0	0	0	6	6	14.4
Reaction wheel 3	0	0	0	0	0	6	6	14.4
Reaction wheel 4	0	0	0	0	0	6	6	14.4
Magneto_Torquer -Y	0	1.2	1.2	3	3	2.16	2.16	0
TRI-TEL S	0	0	0	0	0	0	0	0
TMTC Antenna + Y	0	0	0	0	0	0	0	0
TMTC box	0	12	33.6	12	33.6	12	33.6	12
Gyro box	0	0	0	0	0	13.2	13.2	13.2
Magnetometer 1	0	1.44	1.44	1.44	1.44	1.44	1.44	1.44
Magnetometer 2	0	1.44	1.44	1.44	1.44	1.44	1.44	1.44
TMTC Antenna +Z	0	0	0	0	0	0	0	0
EPS Battery	0	0	0	0	0	0	0	0
LMP	0	0	0	0	0	0	0	0
Magneto_Torquer - Z	0	1.2	1.2	3	3	2.16	2.16	0
TMTC Antenna -Z	0	0	0	0	0	0	0	0

Table 11. Operational modes [Dissipated Power Modes 9-15]

Component	Mode9	Mode10	Mode11	Mode12	Mode13	Mode14	Mode15
AMSAT box	0	0	0	0	0	0	0
TMTC Redundant	0	0	0	0	0	0	0
TMTC antenna +X	0	0	0	0	0	0	0
OBDH	30	30	30	30	30	30	30
EPS PEB	12	12	12	12	12	12	12
Star tracker	0	0	0	0	0	4.8	4.8
TMTC antenna -X	0	0	0	0	0	0	0
Reaction Wheel	0	0	0	0	0	0	0
UCAM	3.6	0	0	3.6	3.6	0	0
Magneto-Torquer +Y	0	0	0	0	0	2.16	2.16
TMTC Antenna +Y	0	0	0	0	0	0	0
Reaction wheel 1	14.4	8.4	8.4	14.4	14.4	6	6
Reaction wheel 2	14.4	8.4	8.4	14.4	14.4	6	6
Reaction wheel 3	14.4	8.4	8.4	14.4	14.4	6	6
Reaction wheel 4	14.4	8.4	8.4	14.4	14.4	6	6
Magneto_Torquer -Y	0	0	0	0	0	2.16	2.16
TRI-TEL S	0	8.4	8.4	8.4	8.4	0	0
TMTC Antenna + Y	0	0	0	0	0	0	0
TMTC box	33.6	12	33.6	12	33.6	12	33.6
Gyro box	13.2	13.2	13.2	13.2	13.2	13.2	13.2
Magnetometer 1	1.44	1.44	1.44	1.44	1.44	1.44	1.44
Magnetometer 2	1.44	1.44	1.44	1.44	1.44	1.44	1.44
TMTC Antenna +Z	0	0	0	0	0	0	0
EPS Battery	0	0	0	0	0	0	0
LMP	0	6	6	6	6	0	0
Magneto_Torquer - Z	0	0	0	0	0	2.16	2.16
TMTC Antenna -Z	0	0	0	0	0	0	0

Table 12. Operational modes [Dissipated Power Modes 16-22]

Component	Mode16	Mode17	Mode18	Mode19	Mode20	Mode21	Mode22
AMSAT box	0	0	54.84	54.84	0	0	0
TMTC Redundant	0	0	0	0	0	0	0
TMTC antenna +X	0	0	0	0	0	0	0
OBDH	30	30	30	30	30	30	30
EPS PEB	12	12	12	12	12	12	12
Star tracker	0	0	0	0	0	0	0
TMTC antenna -X	0	0	0	0	0	0	0
Reaction Wheel	3.3	3.3	0	0	0	0	0
UCAM	0	0	0	0	0	0	0
Magneto-Torquer +Y	2.16	2.16	2.16	2.16	2.16	2.16	0
TMTC Antenna +Y	0	0	0	0	0	0	0
Reaction wheel 1	6	6	6	6	12	12	14.4
Reaction wheel 2	6	6	6	6	12	12	14.4
Reaction wheel 3	6	6	6	6	12	12	14.4
Reaction wheel 4	6	6	6	6	12	12	14.4
Magneto_Torquer -Y	2.16	2.16	2.16	2.16	2.16	2.16	0
TRI-TEL S	0	0	0	0	0	0	0
TMTC Antenna + Y	0	0	0	0	0	0	0
TMTC box	12	33.6	12	33.6	12	33.6	12
Gyro box	13.2	13.2	13.2	13.2	0	0	13.2
Magnetometer 1	1.44	1.44	1.44	1.44	1.44	1.44	1.44
Magnetometer 2	1.44	1.44	1.44	1.44	1.44	1.44	1.44
TMTC Antenna +Z	0	0	0	0	0	0	0
EPS Battery	0	0	0	0	0	0	0
LMP	0	0	0	0	0	0	0
Magneto_Torquer - Z	2.16	2.16	2.16	2.16	2.16	2.16	0
TMTC Antenna -Z	0	0	0	0	0	0	0

Table 13. Operational modes [Dissipated Power Modes 23-26]

Component	Mode23	Mode24	Mode25	Mode26
AMSAT box	0	0	0	54.84
TMTC Redundant	0	0	0	0
TMTC antenna +X	0	0	0	0
OBDH	30	30	30	30
EPS PEB	12	12	12	12
Star tracker	0	0	0	0
TMTC antenna -X	0	0	0	0
Reaction Wheel	0	0	0	0
UCAM	0	0	0	0
Magneto-Torquer +Y	0	1.08	1.08	1.08
TMTC Antenna +Y	0	0	0	0
Reaction wheel 1	14.4	0	0	0
Reaction wheel 2	14.4	0	0	0
Reaction wheel 3	14.4	0	0	0
Reaction wheel 4	14.4	0	0	0
Magneto_Torquer -Y	0	1.08	1.08	1.08
TRI-TEL S	0	0	0	0
TMTC Antenna + Y	0	0	0	0
TMTC box	33.6	12	33.6	0
Gyro box	13.2	0	0	0
Magnetometer 1	1.44	1.44	1.44	1.44
Magnetometer 2	1.44	1.44	1.44	1.44
TMTC Antenna +Z	0	0	0	0
EPS Battery	0	0	0	0
LMP	0	0	0	0
Magneto_Torquer - Z	0	1.08	1.08	1.08
TMTC Antenna -Z	0	0	0	0

7. Thermal Control Design

This analysis is conducted using Thermal Desktop (TD) software, which supports both finite difference and finite element methods and can be used with or without graphical interfaces. The analysis begins by collecting overall data on the nominal operating temperature ranges and expected heat dissipation of the satellite's equipment. Additionally, it is essential to define the thermal boundary conditions.

The ESEO thermal control system was originally designed as passive and active thermal control elements, with thermal analysis conducted using the ESATAN software package. Passive thermal control elements are tapes, coatings, radiators, and Multi-Layer Insulation (MLI) applied to the satellite to control radiation heat exchange between the satellite and its environment, and Active thermal control element is heaters to compensate heat in cold case.

All thermal analyses consider two temperature limits [13]:

Allowable Operative Temperature: The device works efficiently within a specific temperature range, which differs depending on its function and application. This range covers from the minimum operating temperature to the maximum operating temperature. If the temperature moves afar this range, the device no longer meets its functional specifications and may fail.

Allowable Fail Temperature: If the device goes above its operative temperature range, it will not function correctly but remains structurally unbroken. However, if the temperature surpasses the fail temperature limit, the component will have permanent failure.

8. Results

The external heat flux incident on the spacecraft's external surfaces throughout one orbit is calculated for 81 nodes using Thermal Desktop in both sun-pointing and nadir-pointing modes. The results are then compared with corresponding analyses from ESATAN.

The distribution of external fluxes on the spacecraft is primarily influenced by orientation changes during the orbit. Table (14) expresses cases definition on-orbit thermal analysis as shown;

Table 14. On-orbit thermal analysis case definition

Environmental Condition	Analysis Case	Operating
Hot Case	Case 1	Sun Pointing
	Case 2	Nadir
Cold Case	Case 3	Sun Pointing
	Case 4	Nadir

Transient thermal analysis studies using the Thermal Desktop model affords important visions into thermal environment impacts on satellite and progresses over several orbits. The results show that after four orbital periods, temperature variations stabilize that means the satellite follows expected thermal cycle in later orbits. Solar panels, structural panels, and all internal satellite components temperatures were analyzed.

Table 15 and table 16 shows hot case analysis. Table 15 shows the analysis of case (1) with four sections as mentioned below. The first section illustrates maximum temperature limits for operating temperature and failure temperature, second section illustrates the temperatures variation analysis the case (1) in orbit by both software, third section illustrates the maximum temperature difference and percentage error between structure panels are (2.12°C & 2.12°C) with (Deviation Error = 0.72% & 0.69%) that is panel_3 (+Z) and panel_1 (+X) respectively. The maximum temperature difference between solar panels is (0.88°C) with (Deviation Error = 0.27%) that is solar panel (+Z).

Table 16 shows the analysis of case (2) with four sections as mentioned below. The first section illustrates maximum temperature limits for operating temperature and failure temperature, second section illustrates the temperatures variation analysis for the case (2) in orbit by both software, third section illustrates the maximum temperature difference and percentage error is (2.61°C) with (Error = 0.87%) that is AMSAT in panel_1 (+X). The maximum temperature difference between solar panels is (2.35°C) with (Error = 0.62%) that is solar panel (+X).

Table 15. Hot Case (1) Summary Results

Components	Maximum Temperature [K]				ΔT	Deviation Error %
	Temperature Limits		Temperature Analysis			
	T_{Op}	T_{Fa}	T_{ESATAN}	T_{TDT}		
PANEL 1 (+X)	323	323	290.05	292.15	2.10	0.72
AMSAT	338	373	293.83	295.00	1.17	0.40
GYRO	313	333	276.72	277.24	0.52	0.19
PANEL 2 (+Y)	323	323	312.32	310.20	2.12	0.68
TRITEL	293	343	279.03	277.63	1.40	0.50
UCAM	328	353	317.54	316.34	1.20	0.38
PANEL 3 (+Z)	323	323	308.88	306.76	2.12	0.69
LMP BOX	333	353	319.03	320.85	1.82	0.57
MAGNETOMETER 1	338	353	323.01	324.18	1.17	0.36
MAGNETOMETER 2	338	353	323.01	321.45	1.56	0.48
TMTC REDANDUNT	333	343	319.17	319.30	0.13	0.04
PANEL 4 (-X)	323	323	312.41	312.59	0.18	0.06
OBDH	313	343	296.98	296.55	0.43	0.15
PEB	313	323	302.27	302.98	0.71	0.24
STAR TRACKER	232	343	314.40	314.66	0.26	0.08
TMTC ANTENNA	333	343	324.81	324.13	0.68	0.21
PANEL 5 (-Y)	323	323	301.47	301.94	0.47	0.16
REACTION WHEEL 1	318	333	295.86	294.38	1.48	0.50
REACTION WHEEL 2	318	333	295.86	294.19	1.67	0.56
REACTION WHEEL 3	318	333	295.86	294.63	1.23	0.41
REACTION WHEEL 4	318	333	295.87	294.02	1.85	0.63
MAGNETO TORQUER (-Y)	318	328	296.46	297.23	0.77	0.26
PANEL 6 (-Z)	323	323	315.29	315.55	0.26	0.08
BATTERY	288	293	280.31	280.17	0.14	0.05
TMTC MAIN	333	343	324.81	323.34	1.47	0.45
MAGNETO TORQUER (-Z)	313	328	310.23	310.50	0.27	0.09
SOLAR PANEL (+X)	388	388	323.64	324.30	0.66	0.20
SOLAR PANEL (+Z)	388	388	330.14	331.02	0.88	0.27
SOLAR PANEL (-Z)	388	388	326.65	326.11	0.54	0.17

Table 16. Hot Case (2) Summary Results

Components	Maximum Temperature [K]				ΔT	Deviation Error %
	Temperature Limits		Temperature Analysis			
	T_{Op}	T_{Fa}	T_{ESATAN}	T_{TDT}		
PANEL 1 (+X)	323	323	291.54	290.91	0.63	0.22
AMSAT	338	373	301.32	298.71	2.61	0.87
GYRO	313	333	280.52	278.78	1.74	0.62
PANEL 2 (+Y)	323	323	286.20	285.37	0.83	0.29
TRITEL	293	343	261.15	261.55	0.40	0.15
UCAM	328	353	291.83	290.94	0.89	0.30
PANEL 3 (+Z)	323	323	290.67	290.90	0.23	0.08
LMP BOX	333	353	301.18	301.32	0.14	0.04
MAGNETOMETER 1	338	353	303.22	302.80	0.42	0.14
MAGNETOMETER 2	338	353	303.22	302.34	0.88	0.29
TMTC REDANDUNT	333	343	301.05	300.92	0.13	0.04
PANEL 4 (-X)	323	323	278.15	277.89	0.26	0.09
OBDH	313	343	267.85	267.26	0.59	0.22
PEB	313	323	268.11	268.11	0.00	0.00
STAR TRACKER	323	343	283.74	283.36	0.38	0.14
TMTC ANTENNA	333	343	306.35	306.73	0.38	0.12
PANEL 5 (-Y)	323	323	273.27	273.68	0.41	0.15
REACTION WHEEL 1	318	333	267.62	267.85	0.23	0.09
REACTION WHEEL 2	318	333	267.62	267.54	0.08	0.03
REACTION WHEEL 3	318	333	267.62	267.67	0.05	0.02
REACTION WHEEL 4	318	333	267.62	267.51	0.11	0.04
MAGNETO TORQUER (-Y)	318	328	273.00	271.25	1.75	1.74
PANEL 6 (-Z)	323	323	283.95	283.82	0.13	0.04
BATTERY	288	293	258.09	256.40	1.69	0.65
TMTC MAIN	333	343	293.39	292.58	0.81	0.28
MAGNETO TORQUER (-Z)	318	328	278.45	278.21	0.24	0.09
SOLAR PANEL (+X)	388	388	379.87	377.52	2.35	0.62
SOLAR PANEL (+Z)	388	388	357.93	357.20	0.73	0.20
SOLAR PANEL (-Z)	388	388	341.76	340.50	1.26	0.37

Table 17 and table 18 shows cold case analysis. Table 17 shows the analysis of case (3) with four sections as mentioned below. The first section illustrates minimum temperature limits for operating temperature and failure temperature, second section illustrates the temperatures variation analysis for the case (3) in orbit by both software, third section illustrates the maximum temperature difference and percentage error between structure panels are (0.99℃) with (Error = 0.35%) that is panel_2 (+Y). The maximum temperature difference between solar panels is (1.68℃) with (Error = 0.52%) that is solar panel (+Z).

Table 17. Cold Case (3) Summary Results

Components	Minimum Temperature [K]				ΔT	Deviation Error %
	Temperature Limits		Temperature Analysis			
	T_{Op}	T_{Fa}	T_{ESATAN}	T_{TDT}		
PANEL 1 (+X)	243	243	283.33	283.92	0.59	0.21
AMSAT	233	223	293.63	293.19	0.44	0.15
GYRO	268	248	259.26	260.48	1.22	0.47
PANEL 2 (+Y)	243	243	278.93	277.94	0.99	0.35
TRITEL	243	233	278.76	278.10	0.66	0.24
UCAM	253	228	268.97	268.84	0.13	0.05
PANEL 3 (+Z)	243	243	278.54	278.53	0.01	0.00
LMP BOX	248	228	273.77	273.82	0.05	0.02
MAGNETOMETER 1	253	233	268.89	268.17	0.72	0.27
MAGNETOMETER 2	253	233	268.89	268.56	0.33	0.12
TMTC REDANDUNT	248	238	273.70	274.26	0.56	0.20
PANEL 4 (-X)	243	243	279.55	279.21	0.34	0.12
OBDH	253	238	277.09	277.67	0.58	0.21
PEB	253	243	273.41	273.31	0.10	0.04
STAR TRACKER	253	233	272.17	272.16	0.01	0.00
TMTC ANTENNA	248	238	270.97	271.48	0.51	0.19
PANEL 5 (-Y)	243	243	261.81	261.24	0.57	0.22
REACTION WHEEL 1	253	248	251.85	252.09	0.24	0.10
REACTION WHEEL 2	253	248	251.85	252.07	0.22	0.09
REACTION WHEEL 3	253	248	251.85	252.00	0.15	0.06
REACTION WHEEL 4	253	248	251.85	251.87	0.02	0.01
MAGNETO TORQUER (-Y)	243	233	261.83	261.41	0.42	0.16
PANEL 6 (-Z)	243	243	275.74	275.61	0.13	0.05
BATTERY	273	268	245.77	244.27	1.50	0.61
TMTC MAIN	248	238	270.97	271.70	0.73	0.27
MAGNETO TORQUER (-Z)	243	233	275.81	275.00	0.81	0.30
SOLAR PANEL (+X)	183	183	339.39	339.92	0.53	0.15
SOLAR PANEL (+Z)	183	183	320.73	319.05	1.68	0.52
SOLAR PANEL (-Z)	183	183	322.50	321.53	0.97	0.30

Table 18 shows the analysis of case (4) with four sections as mentioned below. The first section illustrates minimum temperature limits for operating temperature and failure temperature, second section illustrates the temperature variation analysis for the case (4) in orbit by both software, third section illustrates the maximum temperature difference and percentage error between structure panels are (1.49℃) with (Error = 0. 5%) that is panel_2 (+Y). The maximum temperature difference between solar panels is (2.05℃) with (Error = 0.64%) that is solar panel (+X).

Table 18. Cold Case (4) Summary Results

Components	Minimum Temperature [K]				ΔT	Deviation Error %
	Temperature Limits		Temperature Analysis			
	T_{Op}	T_{Fa}	T_{ESATAN}	T_{TDT}		
PANEL 1 (+X)	243	243	289.29	288.35	0.94	0.33
AMSAT	233	223	299.46	300.56	1.10	0.37
GYRO	268	248	264.77	265.07	0.30	0.11
PANEL 2 (+Y)	243	243	294.96	293.47	1.49	0.50
TRITEL	243	233	293.60	293.66	0.06	0.02
UCAM	253	228	284.27	284.26	0.01	0.00
PANEL 3 (+Z)	243	243	292.89	288.89	0.25	0.09
LMP BOX	248	228	288.64	288.89	0.25	0.09
MAGNETOMETER 1	253	233	283.28	282.94	0.34	0.12
MAGNETOMETER 2	253	233	283.28	282.72	0.56	0.20
TMTC REDANDUNT	248	238	288.32	288.59	0.27	0.09
PANEL 4 (-X)	243	243	305.50	304.09	1.41	0.46
OBDH	253	238	296.60	296.12	0.48	0.16
PEB	253	243	296.18	295.35	0.83	0.28
STAR TRACKER	253	233	302.98	301.86	1.12	0.37
TMTC ANTENNA	248	238	413.61	413.77	0.16	0.04
PANEL 5 (-Y)	243	243	292.87	292.73	0.14	0.05
REACTION WHEEL 1	253	248	283.00	283.19	0.19	0.07
REACTION WHEEL 2	253	248	283.00	283.02	0.02	0.01
REACTION WHEEL 3	253	248	283.00	283.16	0.16	0.06
REACTION WHEEL 4	253	248	283.00	282.84	0.16	0.06
MAGNETO TORQUER (-Y)	243	233	293.00	291.95	1.05	0.36
PANEL 6 (-Z)	243	243	304.57	303.14	1.43	0.47
BATTERY	273	268	271.72	272.02	0.30	0.11
TMTC MAIN	248	238	301.60	302.26	0.66	0.22
MAGNETO TORQUER (-Z)	243	233	304.03	303.50	0.53	0.18
SOLAR PANEL (+X)	183	183	319.32	321.37	2.05	0.64
SOLAR PANEL (+Z)	183	183	317.09	319.00	1.91	0.60
SOLAR PANEL (-Z)	243	243	289.29	288.35	0.94	0.33

9. Conclusion

This study confirms that spacecraft thermal behaviour follows a periodic pattern during each orbit. The external heat flux incident on the spacecraft's external surfaces throughout one orbit is calculated for 81 nodes using Thermal Desktop in both sun-pointing and nadir-pointing modes. The results are then compared with the previous analyses from ESATAN. The Environmental conditions (hot case, cold case) were analysed. Hot case was analysed in two cases [case (1) sun pointing and case (2) nadir pointing] and so as cold case. The results show that:

1- Hot case (sun pointing): the maximum temperature difference between structure panels is 2.12 ℃ with maximum error is 0.72% in panel_3 (+Z) and same temperature difference value with maximum error is 0.69% in panel_1 (+X). The maximum temperature difference between solar panels is 0.88 ℃ with maximum error is 0.27% in solar panel (+Z).

2- Hot case (nadir pointing): the maximum temperature difference between structure panels is 0.83 ℃ with maximum error is 0.29% in panel_2 (+Y). The maximum temperature difference between solar panels is 2.35 ℃ with maximum error is 0.62% in solar panel (+X).

3- Cold case (sun pointing): the maximum temperature difference between structure panels is 0.99 ℃ with maximum error is 0.35% in panel_2 (+Y). The maximum temperature difference between solar panels is 1.68 ℃ with maximum error is 0.52% in solar panel (+Z).

4- Cold case (nadir pointing): the maximum temperature difference between structure panels is 1.49 ℃ with maximum error is 0.5% in panel_2 (+Y). The maximum temperature difference between solar panels is 2.05 ℃ with maximum error is 0.64% in solar panel (+X).

References

[1] Ahmed Kamal Mohamed El Hefnawy, "Spacecraft Thermal control," Msc. Thesis. Cairo 2019.

[2] M. Donabedian, "Spacecraft Thermal Control Handbook, Volume II: Cryogenics," 2004. DOI: 10.2514/4.989148.

[3] NASA. State of the Art of small spacecraft technology, February 12, 2024. [Online]. Available: https://www.nasa.gov/smallsat-institute/sst-soa/thermal-control/.

[4] National Aeronautics and Space Administration, "What are SmallSats and CubeSats?," 2017. [Online]. Available: https://www.nasa.gov/content/what-are-smallsats-and-cubesats.

[5] Ahmed Elhefnawy, Ali Elmaihy, Ahmed Elweteedy, "Passive thermal control design and analysis of a university-class satellite". Journal of Thermal Analysis and Calorimetry. Published: 24 August 2022.

[6] Naoko Iwata, Masanori Saitoh, Keiichi Yanagase, Yasuhiro Iso and Yukio Inoue, Hiroyuki Ogawa and Yoshiro Miyazaki, "Thermal and Structural Performance of a Small Satellite with Networked Oscillating Heat Pipes". JOURNAL OF SPACECRAFT AND ROCKETS, Vol. 59, No. 3, May–June 2022.

[7] Tae-Yong Park, Bong-Geon Chae, Hongrae Kim, Kyung-Rae Koo, Sung-Chan Song and Hyun-Ung Oh, "New Thermal Design Strategy to Achieve an 80-Kg-Class Lightweight X-Band Active SAR Small Satellite S-STEP" Aerospace 2021. 8, 278.

[8] Ji-Seok Kim and Hae-Dong Kim. "Thermal Model Correlation and Validation of a 6U Nanosatellite with Multiple Payloads". The Korean Society for Aeronautical & Space Sciences 2021. International Journal of Aeronautical and Space Sciences (2022) 23:207–220.

[9] Luis A. Reyesa,, Roberto Cabriales-Gómez, Carlos E. Chávez, B. Bermúdez-Reyes, Omar López-Botello, P. Zambrano-Robledo, "Thermal modeling of CIIIASat nanosatellite: A tool for thermal barrier coating selection" j.applthermaleng.2019.114651.

[10] N Athanasopoulos, J Farmasonis and NJ Siakavellas, "Preliminary design and comparative study of thermal control in a nanosatellite through smart variable emissivity surfaces" University of Patras. Patras. Achaia 26500. Greece.

[11] Hemant Ganti, Aniketh Ajay Kumar, Arnav Saikia, Anirudh P Kailaje, Akash Paliya, Rohan Sonkusare and Atharva Tikle, "Design of Thermal Model and Implementation of Thermal Solutions for Nano Satellite", 978-1-5090-1613-6/17/$31.00 ©2017 IEEE.

[12] Andreas Berggren, "Design of Thermal Control System for the Spacecraft MIST," Msc. Thesis. KTH Royal Institute of Technology, June 2015.
[13] Michel Jean-Louis Chris Poucet, "Phase-B Thermal Control Subsystem Design for the ESEO Satellite," Msc. Thesis. no. POLITECNICO DI MILANO, 2012.
[14] Isidoro Martínez, "Space Thermal" and "SPACECRAFT THERMAL MODELLING AND TESTING". ETSIAE-UPM. Ciudad Universitaria. E-28040-Madrid. [Online]. Available: http://imartinez.etsiae.upm.es/
[15] Ahmed Elhefnawy, Ali Elmaihy, Ahmed Elweteedy, "A University Small Satellite Thermal Control Modeling and Analysis in the Post-Mission Phase". FME Transactions. VOL. 49, No 4, 2021 ▪ 1017
[16] Ahmed Kamal Mohamed El Hefnawy, "Spacecraft Thermal control" Msc. Thesis. Military Technical college. 2019.
[17] Cihan ATAR, Metin AKTAS, "Advances in Thermal Modeling and Analysis of Satellites". GU J Sci. 35 (1): 42-58 (2022)